

# Characterization of strain at Ga<sub>1-x</sub>Al<sub>x</sub>As-GaAs interfaces using electrolyte electroreflectance

F. H. Pollak<sup>a)</sup>

*Physics Department, Brooklyn College of CUNY, Brooklyn, New York 11210*

J. M. Woodall

*IBM Thomas J. Watson Research Center, Yorktown Heights, New York 10598*

(Received 25 February; accepted 2 May 1980)

Utilizing electrolyte electroreflectance we have been able to detect the strains at the interface of epitaxial Ga<sub>1-x</sub>Al<sub>x</sub>As ( $x \sim 0.9$ ) grown on a GaAs substrate. Use has been made of the fact that the Ga<sub>1-x</sub>Al<sub>x</sub>As is transparent in the wavelength region (1.3–1.9 eV) corresponding to the direct gap (and the spin-orbit split component) of GaAs. The sensitive technique of electrolyte electroreflectance has thus enabled us to “see through” the Ga<sub>1-x</sub>Al<sub>x</sub>As and to observe the properties of the GaAs in the interfacial region. Structures of *p-p-n* Ga<sub>1-x</sub>Al<sub>x</sub>As-GaAs-GaAs solar cell material were prepared using three different modifications of the liquid phase epitaxy method. These various growth conditions produced different interfacial strains which have been observed in shifts of the GaAs substrate electroreflectance spectra. Above 2.5 eV we have observed electroreflectance structure corresponding to the Ga<sub>1-x</sub>Al<sub>x</sub>As epitaxial layer. These optical features have yielded information about the properties of the Ga<sub>1-x</sub>Al<sub>x</sub>As material.

PACS numbers: 68.55. + b, 81.10. — h, 78.20.Hp

## I. INTRODUCTION

Semiconductor heterojunctions and structures are currently a topic of great practical and theoretical interest. In the past decade lattice matched heterojunctions have played a key role in the development of devices such as cw room temperature injection lasers and high efficiency solar cells.<sup>1,2</sup> More recently, attempts to utilize the properties associated with band gap discontinuities at heterojunctions have required very stringent growth conditions during the formation of hetero-

junctions.<sup>1</sup> Of particular interest are the transport properties of very abrupt heterojunctions in materials which have nearly matched lattice constants and thermal expansion coefficients. In order to understand the properties of such junctions it is necessary to have methods which characterize the junction region. It is the purpose of this paper to describe a new technique which characterizes some of the important parameters of heterojunctions.

Utilizing electrolyte electroreflectance (EER) it has been possible to detect the strains at the interface of epitaxial

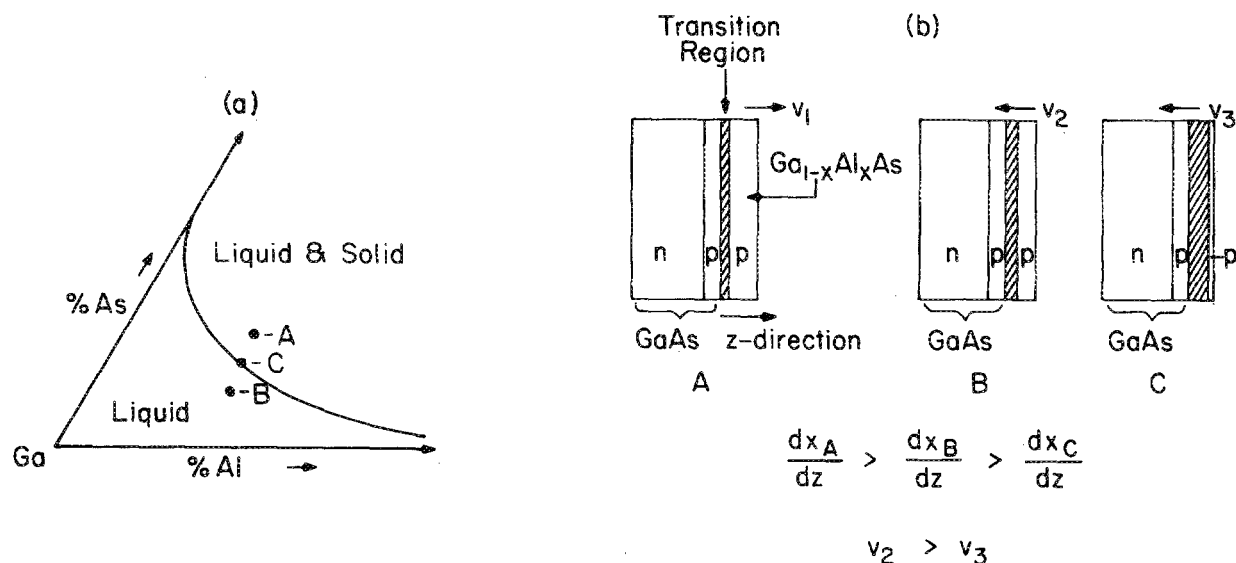


FIG 1. (a) Schematic representation of the phase diagram for the liquid phase epitaxial growth conditions used for the Ga<sub>1-x</sub>Al<sub>x</sub>As layers. (b) Schematic drawings of the various regions of the *p-p-n* Ga<sub>1-x</sub>Al<sub>x</sub>As-GaAs-GaAs solar cell structures. Indicated are the relative magnitudes of the concentration gradient  $dx/dz$  for the three cases.

$Ga_{1-x}Al_xAs$  ( $x \sim 0.9$ ) grown on a GaAs substrate. We have made use of the fact that the  $Ga_{1-x}Al_xAs$  is transparent in the wavelength range (1.3–1.9 eV) corresponding to the direct gap (and its spin orbit component) of the GaAs in the interfacial region. In addition the observed EER spectra above 2.5 eV of the  $Ga_{1-x}Al_xAs$  epitaxial layer has yielded information about the properties of this material.

**II. EXPERIMENTAL DETAIL**

The samples used in this study were  $p-p-n-Ga_{1-x}Al_xAs-GaAs-GaAs$  solar cell structures.<sup>2</sup> The structures were prepared using three different modifications of the liquid phase epitaxy (LPE) method. These conditions are illustrated by the schematic phase diagram in Fig. 1(a). To form the structures, GaAs [100] oriented substrates with  $n = 1-2 \times 10^{17} \text{ cm}^{-3}$  are placed in contact with melts of Ga-Al-As doped with Mg to produce a  $p$ -type carrier concentration in the GaAs layer of about  $1 \times 10^{18} \text{ cm}^{-3}$ . The melts have one of the phase conditions A, B, or C. Melts of type A are initially in a solid-liquid two phase region and hence all are supersaturated. When the GaAs substrate contacts type A melts there is a strong driving force for solid phase precipitation, i.e., growth of a  $p$ -type layer of  $Ga_{1-x}Al_xAs$ , at a velocity,  $v_1$ . This gives rise to a relatively thin transition region [see Fig. 1(b)] in which the composition changes from GaAs to  $Ga_{1-x}Al_xAs$  and, hence, produces a relatively high concentration gradient and large strain at the interface. As the  $p$ -type  $Ga_{1-x}Al_xAs$  layer grows, Mg diffuses into GaAs substrate forming a  $p$  region.

Melts of type B are initially undersaturated. When a GaAs substrate contacts this type of melt, the GaAs begins to dissolve into the melt in an attempt to bring the melt to two phase equilibrium. The continuous movement of solid-liquid interface towards the solid direction at a velocity  $v_2$ , produces a situation of diffusion occurring under a moving boundary condition. This growth condition has been treated theoretically for the case of Ga-Al-As melts.<sup>3</sup> The result is that Al diffuses into GaAs along with the Mg dopant and produces a transition region which is thicker than that for type A melts and hence produces a smaller concentration gradient. Thus, lower strain is expected.

Melts of type C are initially at two phase equilibrium.

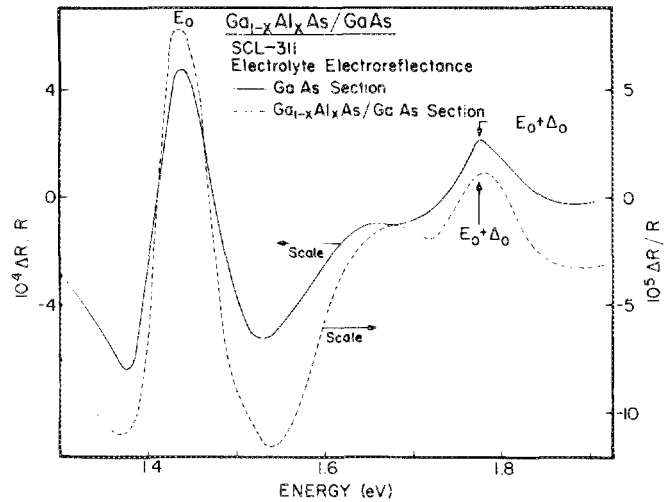


FIG. 2. Electrolyte electroreflectance spectra of sample SCL-311, grown under type C condition, in the energy range 1.3–1.9 eV for the GaAs and  $Ga_{1-x}Al_xAs/GaAs$  sections.

When a GaAs substrate is placed in contact with this melt, dissolution at rate  $v_3$  is also expected to occur but at a lower rate. This results in the widest transition region of the three conditions and hence is expected to produce the lowest strain.

The relative magnitudes of the concentration gradient  $dx/dz$ , for the three growth cases is indicated in Fig. 1(b). In all three instances the combined thickness of the transition region plus the  $Ga_{1-x}Al_xAs$  was about  $1 \mu\text{m}$ .

After growth had been completed the  $Ga_{1-x}Al_xAs$  layer on a portion of the sample was stripped away with HCl in order to expose the GaAs substrate. We shall henceforth refer to this as the GaAs section of the sample and to the unetched region as the  $Ga_{1-x}Al_xAs/GaAs$  section.

The EER technique has been described extensively in the literature.<sup>4</sup> The electrolyte used was a 1:4 solution of glycerol in water. The modulating voltage was in the form of a square wave, 4 V peak-to-peak, at 220 Hz.

The EER measurements were first taken with the light spot on the GaAs section of the sample. Spectra were taken in the vicinity of the  $E_0$  (direct gap at  $k = 0$ ) and  $E_0 + \Delta_0$  (spin-orbit split component) features of GaAs which occur in the energy range 1.3–1.9 eV.<sup>4</sup> For one sample (SCL-311) we have also

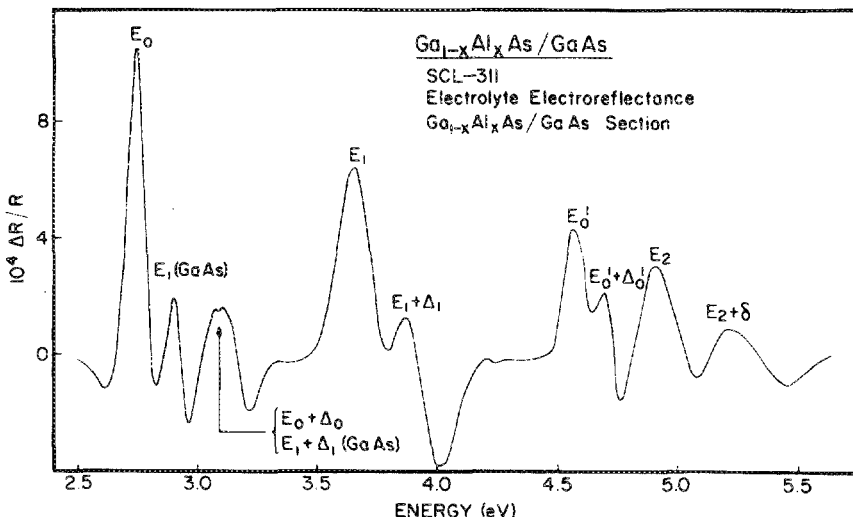


FIG. 3. Electrolyte electroreflectance spectra of the  $Ga_{1-x}Al_xAs-GaAs$  section of sample SCL-311 in the energy range 2.5–5.5 eV.

measured the EER spectra for the GaAs section up to 5.5 eV. The light spot was then moved so that it impinged on the  $\text{Ga}_{1-x}\text{Al}_x\text{As}/\text{GaAs}$  section of the sample. EER measurements were again taken in the range 1.3–1.9 eV as well as at higher photon energies up to 5.5 eV. In the former region the  $\text{Ga}_{1-x}\text{Al}_x\text{As}$  is transparent and hence the EER features observed in this range corresponded to the GaAs at the  $\text{Ga}_{1-x}\text{Al}_x\text{As}/\text{GaAs}$  interface. Features associated with the  $\text{Ga}_{1-x}\text{Al}_x\text{As}$  epitaxial layer were seen above 2.5 eV.<sup>5</sup>

### III. EXPERIMENTAL RESULTS

Shown in Fig. 2 is the EER spectra of sample SCL-311 in the energy range 1.3–1.9 eV for the GaAs and  $\text{Ga}_{1-x}\text{Al}_x\text{As}/\text{GaAs}$  sections of the sample. This sample was grown under the type C condition indicated in Fig. 1. The  $E_0$  and  $E_0 + \Delta_0$  optical structures have been noted and appear at the same positions as previously reported for GaAs.<sup>4</sup> Note that these features for the  $\text{Ga}_{1-x}\text{Al}_x\text{As}/\text{GaAs}$  section occur at the same energy as for the GaAs section. This indicates that there is virtually no strain at the  $\text{Ga}_{1-x}\text{Al}_x\text{As}/\text{GaAs}$  interfacial region since such a strain would shift the positions of these structures.<sup>6</sup> The absence of strain is consistent with the type C growth condition which produces the widest transition region and hence the lowest  $dx/dz$ .

In Fig. 3 we have plotted the EER spectrum of the  $\text{Ga}_{1-x}\text{Al}_x\text{As}/\text{GaAs}$  section of sample SCL-311 in the energy range 2.5–5.5 eV. The  $E_0$  feature of the  $\text{Ga}_{1-x}\text{Al}_x\text{As}$  (direct gap at  $k = 0$ ) occurs at 2.735 eV indicating that  $x = 0.89$  for this material.<sup>5</sup> Note that  $E_0$  peak of the  $\text{Ga}_{1-x}\text{Al}_x\text{As}$  is quite sharp. The feature at 2.90 eV corresponds exactly to the  $E_1$  EER structure that we have observed for the GaAs section of this sample. At energies slightly above the direct gap of  $\text{Ga}_{1-x}\text{Al}_x\text{As}$  the penetration depth is still large enough to enable the light to sense the GaAs at the interface. Since the energy of this structure in Fig. 3 is the same as that for the  $E_1$  feature of the GaAs section, we have obtained a further confirmation of the absence of strain at the interface. In the range 3.0–3.2 eV there is a feature which seems to be a combination of the  $E_0 + \Delta_0$  of the  $\text{Ga}_{1-x}\text{Al}_x\text{As}$  and the  $E_1 + \Delta_1$  of the GaAs substrate. Above 3.2 eV only the features corresponding to the

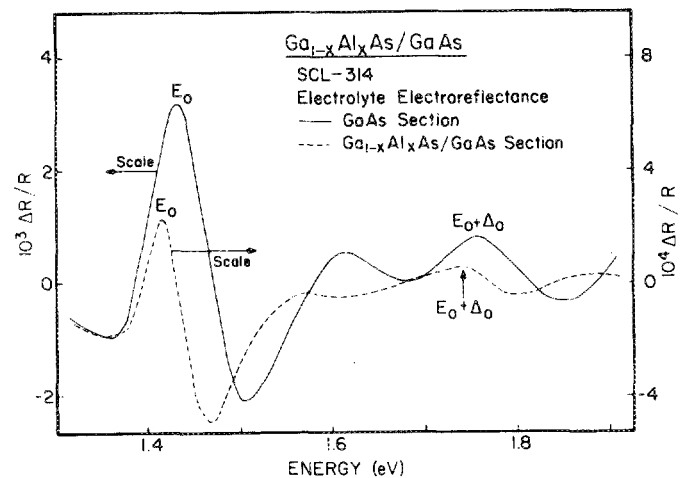


FIG. 4. Electrolyte electroreflectance spectra of sample SCL-314, grown under the type B condition, in the range 1.3–1.9 eV for the GaAs and  $\text{Ga}_{1-x}\text{Al}_x\text{As}/\text{GaAs}$  sections.

$\text{Ga}_{1-x}\text{Al}_x\text{As}$  are observed.<sup>5</sup> It should be pointed out that we have seen the  $E_2 + \delta$  feature<sup>4</sup> which was not reported in Ref. 5.

The EER spectra in the range 1.3–1.9 eV for sample SCL-314 is shown in Fig. 4 for both the GaAs and  $\text{Ga}_{1-x}\text{Al}_x\text{As}/\text{GaAs}$  sections. For this sample the  $\text{Ga}_{1-x}\text{Al}_x\text{As}$  was prepared under the B growth condition illustrated in Fig. 1. In this case the  $E_0$  and the  $E_0 + \Delta_0$  features of the two sections do not occur at the same energy, the structure originating from the  $\text{Ga}_{1-x}\text{Al}_x\text{As}/\text{GaAs}$  interface being shifted to longer wavelengths by  $\sim 20$  meV. This shift to lower energies indicates that the strain is tensile.<sup>6</sup> Based on the deformation potentials of the  $E_0$  and  $E_0 + \Delta_0$  gaps and the elastic constants of GaAs<sup>7</sup> we estimate the strain to be  $\sim 0.1\%$ . This value contains an uncertainty of about a factor of 2 which is dependent upon the assumptions made regarding the nature of the interfacial strain, i.e., hydrostatic, uniaxial or a combination of both. The magnitude and sign of the strain are in good agreement with the mismatch in lattice constants between GaAs and  $\text{Ga}_{1-x}\text{Al}_x\text{As}$ <sup>1</sup> and are consistent with the growth conditions.

Plotted in Fig. 5 is the EER spectrum of the  $\text{Ga}_{1-x}\text{Al}_x\text{As}/\text{GaAs}$  section of sample SCL-314 in the energy range 2.5–5.5

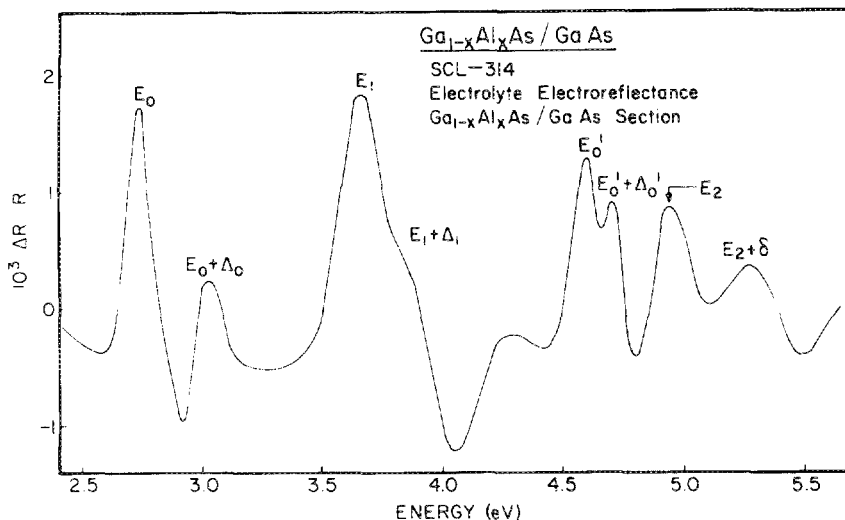


FIG. 5. Electrolyte electroreflectance spectra of the  $\text{Ga}_{1-x}\text{Al}_x\text{As}/\text{GaAs}$  section of sample SCL-314 in the energy range 2.5–5.5 eV.

eV. The  $E_0$  feature occurs at 2.735 eV, the same energy as that for the SCL-311 sample (see Fig. 3). This shows that the different growth conditions produce the same value of the composition  $x$  in the region of the penetration depth of the  $E_0$  structure. Figure 5 also shows that the  $E_0$  feature for sample SCL-314 is broader than that for sample SCL-311.

For sample SCL-314 the  $E_1$  and  $E_1 + \Delta_1$  features are not resolved (see Fig. 5). We attribute this effect to the following cause. For melt  $B$  conditions it is observed that the GaAs does not dissolve in a uniform manner. Rather, the planar interface breaks up into somewhat periodic regions of ridges and valleys. The thickness of the  $\text{Ga}_{1-x}\text{Al}_x\text{As}$  layer and transition region varies between ridge and valley areas. This will produce a "smearing out" of the EER spectra at energies where the penetration depth ( $\sim 200\text{--}300 \text{ \AA}$  for the  $E_1$  and  $E_1 + \Delta_1$  peaks)<sup>8</sup> will sample regions of the  $\text{Ga}_{1-x}\text{Al}_x\text{As}$  having steep profiles. Since  $E_0$ ,  $E_0 + \Delta_0$  EER features of sample SCL-314 are resolved the above effect is not occurring within  $\sim 70 \text{ \AA}$  of the surface<sup>8</sup> but only at the depth of  $\sim 200\text{--}300 \text{ \AA}$ .

The  $E_0$  and  $E_0 + \Delta_0$  EER spectra of the GaAs and  $\text{Ga}_{1-x}\text{Al}_x\text{As}/\text{GaAs}$  sections of sample SCL-326 are shown in Fig. 6. This material was prepared under the type A growth condition (see Fig. 1) and should have the largest interfacial strains. The  $E_0 + \Delta_0$  optical peak of the  $\text{Ga}_{1-x}\text{Al}_x\text{As}/\text{GaAs}$  section is shifted to lower energies by  $\sim 60 \text{ meV}$  in relation to the corresponding peak of the GaAs section. This indicates that the tensile strain in the interfacial region for this sample is about a factor of 3 larger than for the SCL-314 material (see Fig. 4).

The  $E_0$  feature has a considerable amount of structure for both the  $\text{Ga}_{1-x}\text{Al}_x\text{As}/\text{GaAs}$  and GaAs sections. At present we do not understand this effect. It may be due to the greater strain introduced by the type A growth method which produces a splitting of the degenerate valence band edge of the GaAs<sup>6</sup> on the interfacial region. We may also be seeing this effect on the GaAs section due to incomplete etching which has left some residual strain. These aspects are being pursued further.

Figure 7 displays the EER spectrum of the  $\text{Ga}_{1-x}\text{Al}_x\text{As}/\text{GaAs}$  of sample SCL-326 in the range 2.5–5.5 eV. The  $E_0$  peak

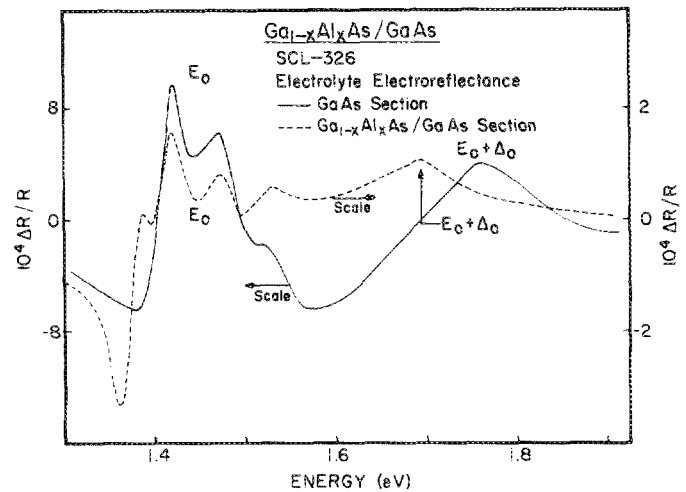


FIG. 6. Electrolyte electroreflectance spectra of sample SCL-326, grown under the type A condition, in the range 1.3–1.9 eV for the GaAs and  $\text{Ga}_{1-x}\text{Al}_x\text{As}/\text{GaAs}$  sections.

is at the same energy as for the other two materials. The  $E_1$  and  $E_1 + \Delta_1$  features are resolved indicating that the effect described above for the type B growth procedure does not occur in this case.

#### IV. CONCLUSIONS

The results of this study clearly demonstrate the usefulness of the electroreflectance method for determining differences in semiconductor heterojunctions. In addition it shows the strong dependence of the properties of heterojunctions on small changes in the LPE method. This is an important point especially with respect to injection lasers, where small changes in interface properties can effect device yield, performance, and operating lifetime. Thus a goal of future studies might be an attempt to find a correlation of electroreflectance characterization with device performance.

Interfacial strains in thin films can also be determined by x-ray topography techniques.<sup>9</sup> The lower limit of these measurements is reported to be about  $10^9 \text{ dynes/cm}^2$  for films

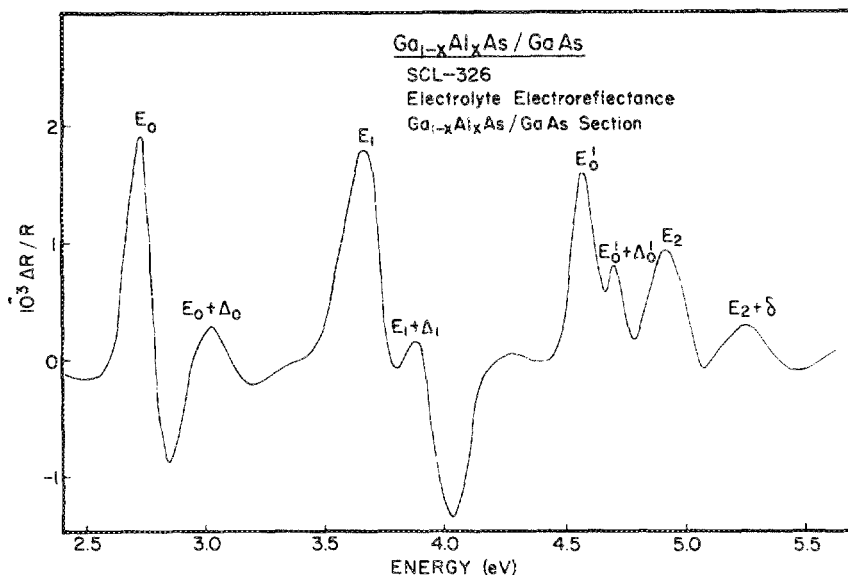


FIG. 7. Electrolyte electroreflectance spectra of the  $\text{Ga}_{1-x}\text{Al}_x\text{As}/\text{GaAs}$  section of sample SCL-326 in the energy range 2.5–5.5 eV.

1000 Å thick. Our technique is somewhat more sensitive. For example, Fig. 4 shows a shift of about 20 meV which corresponds to a stress of  $\sim 2 \times 10^9$  dynes/cm<sup>2</sup>.<sup>6</sup> We could easily detect a shift of several meV and hence stresses of  $\sim 5 \times 10^8$  dyn/cm<sup>2</sup>. In addition the sensitivity of our method is independent of film thickness which is not true for the x-ray topography methods.<sup>9</sup>

### ACKNOWLEDGMENTS

Fred H. Pollak wishes to acknowledge the support of the Office of Naval Research under contract N000 14-78-C-0890 and the National Science Foundation under grant DMR-78-03030.

<sup>a</sup>IBM Summer Faculty Research Participant 1979

<sup>1</sup>See, for example, A. G. Milnes and D. L. Feucht, *Heterojunctions and Metal-Semiconductor Junctions* (Academic, New York, 1972).

<sup>2</sup>See, for example, H. Hovel, *Solar Cells, Semiconductor and Semimetals*, Vol. 11 (Academic, New York, 1975).

<sup>3</sup>M. B. Small and R. Ghez, *J. Appl. Phys.* **50**, 5322 (1979).

<sup>4</sup>See, for example, Y. Hamakawa and T. Nishino, in *Optical Properties of Solids—New Developments*, edited by B. O. Seraphin (North-Holland, Amsterdam, 1976).

<sup>5</sup>O. Berolo and J. C. Wooley, *Can. J. Phys.* **49**, 1335 (1971).

<sup>6</sup>M. Chandrasekhar and F. H. Pollak, *Phys. Rev.* **15**, 2127 (1977).

<sup>7</sup>See, for example, O. Madelung, *Physics of III-V Compounds* (Wiley, New York, 1964) p. 345.

<sup>8</sup>For the III-V materials the penetration depth of the light in the vicinity of the  $E_1$  and  $E_1 + \Delta_1$  features is typically  $\sim 200$ – $300$  Å while for the  $E'_0$  and  $E'_0 + \Delta'_0$  peaks it is  $\sim 70$  Å. See, for example, B. O. Seraphin and H. E. Bennett in *Semiconductors and Semimetals*, Vol. 3 (Academic, New York, 1967), p. 499.

<sup>9</sup>See, for example, E. W. Hearn in *Advances in X-Ray Analysis*, edited by H. F. McMurdie, C. S. Barrett, J. B. Newkirk and C. O. Ruud (Plenum New York 1977) Vol. 20, p. 273.